


Article

Effect of Interior Space and Window Geometry on Daylighting Performance for Terrace Classrooms of Universities in Severe Cold Regions: A Case Study of Shenyang, China

Yingjie Jia, Zheming Liu * , Yaoxuan Fang, Huiying Zhang, Caiyi Zhao and Xuqiang Cai

Jangho Architecture College, Northeastern University, Shenyang 110819, China

* Correspondence: liuzheming@mail.neu.edu.cn

Abstract: Good daylighting performance positively affects students' physical and mental health, learning efficiency, and the building's energy-saving capability. Due to the terrace classroom having ample space, large capacity, the ability to avoid obstructing sight, and the ability to meet various use needs, it is the most important place in university buildings. However, research on the daylighting performance of university terrace classrooms is limited, leading to a lack of quantitative guidance in early design stages. This study aims to explore the effects of interior space and window geometry of terrace classrooms in universities in severe cold regions on daylighting performance. This research took Shenyang as an example; spatial daylight autonomy (sDA_{300,50%}) and useful daylight illuminance (UDI_{100–2000}) were selected as daylighting performance evaluation indices. Based on the Grasshopper parametric platform, the simulation was carried out using Ladybug and Honeybee plugins. Correlation and regression analyses revealed the relationship between interior space and window geometry parameters and the evaluation indices. The results showed the following: window-to-floor ratio (WFR), classroom height (H_{tc}), window height (H_w), window-to-wall ratio (WWR), classroom width (W_{tc}), and window width (W_w) have positive effects on improving the daylight sufficiency of the terrace classrooms facing each orientation, and the degree of the effect decreases in order. To ensure the overall daylighting performance, the W_{tc} can be maximized. The width of walls between windows for south-facing and west-facing classrooms should be 0.9 m. The WWR and WFR for south-facing classrooms should be 0.3–0.5 and 0.11–0.14, respectively. The WWR and WFR for north-facing classrooms should be 0.6–0.7 and 0.14–0.20, respectively. Prediction models are established for the sDA_{300,50%} and UDI_{100–2000} of the terrace classrooms facing each orientation.

Keywords: daylighting performance; terrace classrooms; interior space geometry; window geometry; severe cold regions



Citation: Jia, Y.; Liu, Z.; Fang, Y.; Zhang, H.; Zhao, C.; Cai, X. Effect of Interior Space and Window Geometry on Daylighting Performance for Terrace Classrooms of Universities in Severe Cold Regions: A Case Study of Shenyang, China. *Buildings* **2023**, *13*, 603. <https://doi.org/10.3390/buildings13030603>

Academic Editor: Alessandro Cannavale

Received: 27 January 2023
Revised: 22 February 2023
Accepted: 23 February 2023
Published: 24 February 2023



Copyright: © 2023 by the authors. Licensee MDPI, Basel, Switzerland. This article is an open access article distributed under the terms and conditions of the Creative Commons Attribution (CC BY) license (<https://creativecommons.org/licenses/by/4.0/>).

1. Introduction

Daylighting for buildings is natural and does not exhibit stroboscopic effects while simultaneously being rich in changes, and it exhibits unique and innate advantages that are incomparable to other artificial light sources. Appropriate interior space and window geometry can effectively play the positive role of natural light and provide a comfortable light environment. This is beneficial to the physical and mental health of users. Furthermore, it can improve learning and work efficiency and can also reduce energy consumption [1–3].

Currently, scholars have performed substantial research on the influence of the interior space and window geometry of multi-functional buildings in different areas on daylighting performance [4–6]. Ghisi and Tinker [7] and Susorova et al. [8] studied the impact of window size, orientation, and room geometry on the daylighting performance of office buildings in different climatic zones, such as desert climate, subtropical climate, Mediterranean climate, and temperate broad-leaved forest climate, which aimed to optimize daylighting quality and energy-saving levels. Lee et al.'s research explored the best

window designs of office buildings in five typical climatic zones in Asia (tropical monsoon climate, subtropical monsoon climate, subtropical marine monsoon climate, temperate monsoon climate, and temperate marine monsoon climate), by simulating the influence of window-to-wall ratios and window orientations on natural light. By conducting an analysis on solar radiation and building energy consumption, design guidelines for energy-saving lighting windows were proposed [9]. With the help of field measurements and numerical simulation methods, Omar et al. explored the promotion effect of window geometry, room depth, and other factors on natural light in a university library in the Mediterranean climate zone to enhance daylighting performance [10]. Fan et al. selected a gymnasium in Xiong'an, Beijing, located in the warm temperate continental monsoon climate zone as the research object. They proposed an optimization method for the window design of the stadium facade based on the average illumination, average solar radiation accumulation per hour, and glare index when the stadium was opened in summer [11]. Huang et al. carried out research on the daylighting performance of painting and calligraphy exhibition halls in museums and took daylight factor (DF), DF uniformity, and discomfort glare index (DGI) as evaluation indicators, by comparing and analyzing the daylighting performance of four lighting modes—low side window, high side window, flat skylight, and sawtooth skylight. Huang et al. proposed the window geometry optimization design method [12]. In addition, many studies evaluated the impact of different interior spaces and window geometries on the natural daylighting performance and visual comfort of residential buildings [13–18].

As the central place to carry out educational activities, educational buildings' indoor physical environment quality is closely related to students' physical and mental health, growth, and living quality [19–21]. In addition, a high-quality indoor environment can effectively improve students' learning efficiency and performance, as well as the interaction and social state between teachers and students, which is conducive to students' subsequent professional development and future social development [15,22]. Daylighting environments are essential parts of indoor physical environments. Providing good daylighting conditions can create a good development environment for students. Therefore, daylighting performance in educational buildings has attracted significant attention. Currently, many research studies on the light environment of educational buildings emphasize improving environment quality and energy-saving levels. Only a few research studies focus on evaluating and improving the natural light environment [23], mainly concentrating on ordinary classrooms, professional classrooms, and laboratories [19,24]. Pellegrino et al. evaluated the daylighting performance of ordinary classrooms in an Italian school with the hope of providing reasonable solutions to improving daylight availability [25]. Rubies et al. took an academic classroom in L'Aquila University as a case to explore the influence of interior space and window geometry on daylighting performance and building lighting energy consumption, by simulating and analyzing parameters such as room geometry, window-to-floor ratio, window shape, window orientation, etc. [26]. Ashrafian and Moazzen selected west-facing and east-facing classrooms in a temperate continental climate zone for simulation to explore whether the average illuminance provided under different window-to-wall ratios met the needs of users; they obtained a window geometry design method that is beneficial for lighting energy saving [22]. Moreover, most regions selected for existing research studies on educational buildings are in middle and low latitudes, such as tropical or warm and humid climates, which makes it difficult to apply the relevant research results to areas with different climates or latitudes [27–30].

With the expansion in enrollment observed in Chinese universities, teaching locations that are spacious and have large capacities are needed to meet the increasing number of students and diversified use needs. Terrace classrooms have the following advantages: A large area, a large number of people, and a stepped floor, which can meet the requirement for more indoor seats and avoid the problem of vision blocking. As the most important teaching location in universities, a terrace classroom's use functions are flexible and changeable and can be used as the principal space for students' self-study, examination, meetings, and community activities. Therefore, the terrace classroom has become the most frequently

used classroom type for university students. The quality of its daylighting performance is of great significance for meeting the needs of students' study life, maintaining physical and mental health, and reducing building energy consumption.

However, currently, the research on the natural light environment of terrace classrooms needs to be improved, and most existing research studies are aimed at artificial lighting and energy consumption [31,32]. In addition, China's related standards and design datasets lack specific guidance strategies for daylighting design in terrace classrooms. Therefore, in order to improve the daylighting performance of university terrace classrooms so that they can play a positive role in students' learning and life and saving architectural lighting energy consumption, it is urgent to study the daylighting performance of university terrace classrooms and propose corresponding design suggestions [33].

China's severe cold regions have higher latitudes and long cold winters. The total illuminance and sunshine hours are fewer than in other areas, so it is necessary to improve the utilization rate of sunlight and play an active role in natural daylighting. Thus, improving the daylighting performance of terrace classrooms in severe cold regions has become an urgent problem. This paper aims to study the relationship between interior space and window geometry and the daylighting performance of university terrace classrooms in severely cold areas. Based on the Grasshopper parameterization platform, the daylighting performance simulation used the Ladybug and Honeybee plug-in in Shenyang, China. Via correlation analysis, box diagram analysis, and multiple linear regression analysis, quantitative analyses were conducted on the relationship between all terrace classroom orientations: (1) Interior space geometry parameters include the following: classroom width (W_{tc}), classroom depth (D_{tc}), and classroom height (H_{tc}). (2) Window geometry parameters include the following: window height (H_w), window width (W_w), number of windows (N_w), the width of wall between windows (W_{wbw}), windowsill height (H_{ws}), window-to-wall ratio (WWR), window-to-floor ratio (WFR), and selected daylighting performance evaluation indices ($sDA_{300,50\%}$ and $UDI_{100-2000}$). Then, the prediction model of the daylighting performance evaluation indices of terrace classrooms facing each orientation was established. The research results provide a reference and evaluation basis for designing university terrace classrooms in severe cold regions.

2. Methodology

2.1. Workflow

The research process mainly includes four steps: (1) problem formulation and objectives; (2) simulation model building, initial parameter setting, and simulation running; (3) parameter analysis and prediction model establishment; (4) description and interpretation (Figure 1).

2.2. Location and Climate

Shenyang is located at $41^{\circ}48'$ northern latitude and $123^{\circ}25'$ eastern longitude, in the south of northeast China and the middle of Liaoning Province. Shenyang has four distinct seasons, with long winters and short summers throughout the year. It belongs to the temperate subhumid continental climate and the severe cold area in China's thermal division [34]. Meteorological data released by the National Meteorological Center (2009–2018) show that the average monthly temperature is $-12\sim 25^{\circ}\text{C}$; the average monthly relative humidity is $49\%\sim 79\%$; and the average temperature in spring, summer, autumn, and winter is $3\sim 16^{\circ}\text{C}$, $18\sim 29^{\circ}\text{C}$, $3\sim 15^{\circ}\text{C}$, and $-15\sim -3^{\circ}\text{C}$, respectively [35].

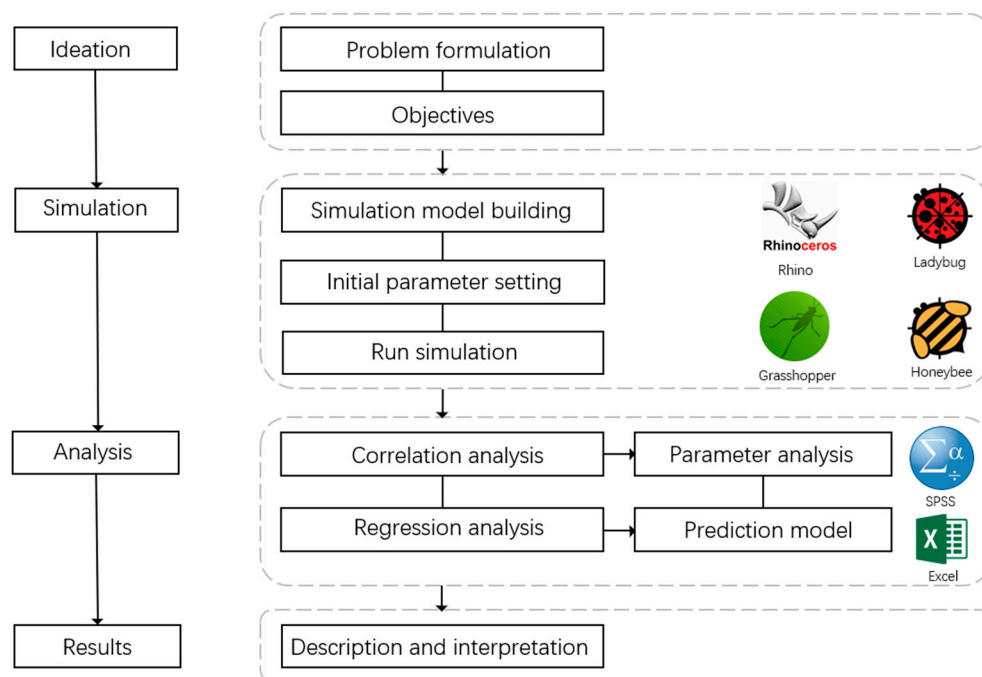


Figure 1. Research workflow.

According to GB 50033-2013 [34] and the annual mean total illuminance obtained by different solar elevation angles, cloud types, cloud cover, and sunshine duration in other regions of China, Shenyang belongs to class III (Figure 2), and the mean total illuminance of natural light years is between 35 and 40 klx. According to the National Meteorological Data Center statistics, the average annual peak sunshine duration was 1406–1582 h in Shenyang from 2000 to 2022. The average annual global horizontal irradiance can reach 5063–5096 MJ/m², and the average annual direct horizontal irradiance can reach 4804–4812 MJ/m² (Figure 3a). The average monthly peak sunshine duration is 64–184 h, the average monthly global horizontal irradiance is 230–663 MJ/m², and the average monthly direct horizontal irradiance is 178–561 MJ/m² (Figure 3b).

2.3. Daylighting Performance Evaluation Criteria

The daylighting performance evaluation index is divided into static and dynamic, forming two types. Among the static daylighting evaluation indices, the daylight factor (DF) is the most widely used index for evaluating light environments [34]. DF lacks orientation and local climate concerns and has been gradually replaced internationally by the more useful daylight illuminance (UDI) and daylight autonomy (DA) indices. Compared with DF, DA reflects the influence of regional photo-climate on the natural lighting performance of buildings and can evaluate their natural lighting level more comprehensively and accurately [36]. Still, DA cannot reflect the proportion of the area reaching the given illuminance in the space. To comprehensively evaluate the DA values of all calculation points, the Illuminating Engineering Society (IES) proposed the sDA index in 2013. If only sDA_{300 lx,50%} is used as the evaluation index, the glare caused by excessive daylighting will be ignored. If only UDI is used as the daylighting performance evaluation index, the adequacy of illuminance cannot be judged [37]. Therefore, this paper selects sDA and UDI as the evaluation indices of daylighting performance.

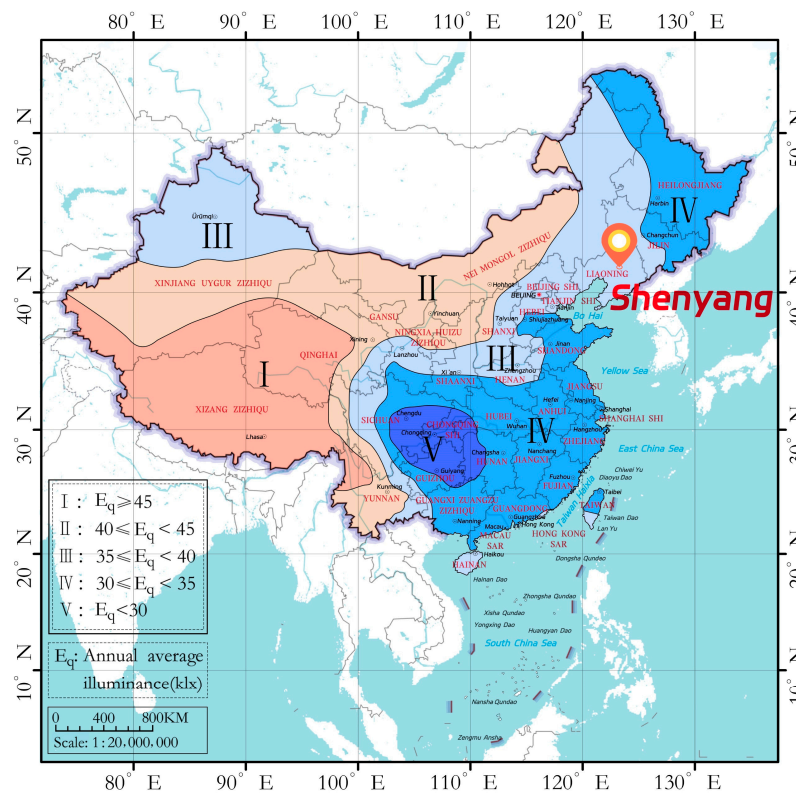


Figure 2. Daylight zone of China.

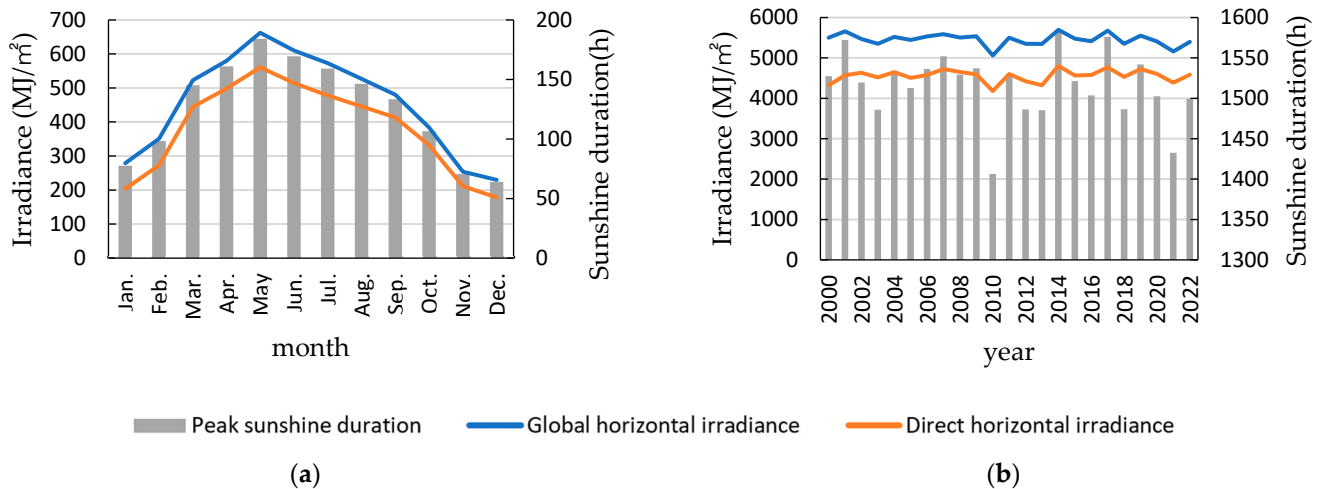


Figure 3. Statistics of solar radiation intensity and peak sunshine duration in Shenyang from 2000 to 2022: (a) mean monthly meteorological data statistics; (b) mean annual meteorological data statistics.

Spatial daylight autonomy (sDA) measures the sufficiency of daylight illuminance in a given area. It is defined as the percentage of the floor area of a building that receives natural light above a specified minimum illuminance value (300 lx for educational buildings) during a specified working period throughout the year (for example, 50% of the time from 8 a.m. to 6 p.m.) [38]. Based on natural illuminance, this dynamic lighting evaluation index specifies the range or percentage of illuminance, which can accurately determine and evaluate the natural illuminance of building spaces [39]. Therefore, $sDA_{300\text{ lx}, 50\%}$ is selected as the evaluation index in this paper. $sDA_{300\text{ lx}, 50\%}$ is the measure recommended by the Illuminating Engineering Society of North America (IES) and LEED. In addition, IES LM-83-12 rated the sufficiency of the ambient daylight available according to $sDA_{300\text{ lx}, 50\%}$. When $sDA_{300\text{ lx}, 50\%}$ is greater than or equal to 75%, the daylight sufficiency of the analysis

area is rated as “preferred”. When $sDA_{300\text{ lx}, 50\%}$ is in the range of 55–75%, the daylight sufficiency of the analysis area is rated as “nominally acceptable”.

Useful daylight illuminance (UDI) represents the frequency at which natural lighting illuminance reaches a certain range throughout the year. The distribution of natural lighting illuminance is divided into three fields: UDI is defined as the available illuminance within the scope of 100–2000 lx, <100 lx is the range of too-low illuminance, and >2000 lx is the range of too-high illuminance [40]. Natural lighting illuminance that is too low leads to low daylight availability, and natural lighting illuminance that is too high easily causes glare and visual discomfort. Therefore, $UDI_{100-2000}$ is selected as the evaluation index in this paper.

2.4. Simulation Settings

2.4.1. Simulation Tools

Based on the Rhino and Grasshopper platforms, Ladybug and Honeybee plug-ins were used to set the simulation parameters, and the Radiance software was used to simulate the optical environment. This daylighting analysis platform is widely used in building daylighting research, and many studies have verified that this platform has good accuracy [41–44].

As a parameter modeling programming tool of the modeling software Rhino [43], Grasshopper runs on the Rhino platform and is one of the mainstream software used in data design. Radiance, a relatively advanced illuminance forecasting tool, was used as the daylight engine in this study. Ladybug is a microclimate analysis plugin software based on the Grasshopper parameterized platform. The plugin can import EnergyPlus Weather (EPW) data on demand for data analysis and visualization [45]. The Honeybee plug-in can invoke various building performance analysis software for the simulation analysis of natural lighting, thermal comfort, building energy consumption, and output visualization results. This paper used Honeybee to connect Grasshopper to Radiance for the building lighting simulation experiments.

2.4.2. Establishment of Simulation Models

Figure 4 shows the geometric parameter information of the terrace classroom simulation model. This paper determined simulation models by using six parameters, including W_{tc} , D_{tc} , H_w , H_{ws} , W_{wbw} , and the number of walls between windows. According to the relevant provisions in the Architectural Design Data Set [46], the horizontal distance (a) between the front edge of the first step and the front wall of the classroom was set as 5.5 m, the depth of the platform at the back of the classroom was set as 3 m, the slope of the step was set as 9° , and the distance (c) between the upper edge of the window and the ceiling was set as 0.2 m. The width (d) of the window end wall was 1 m [47]. W_{tc} , H_{ws} , and H_w determined H_{tc} . In addition, the windows in the model were evenly distributed horizontally. W_{tc} , W_{wbw} , and the number of walls between the windows determined W_w .

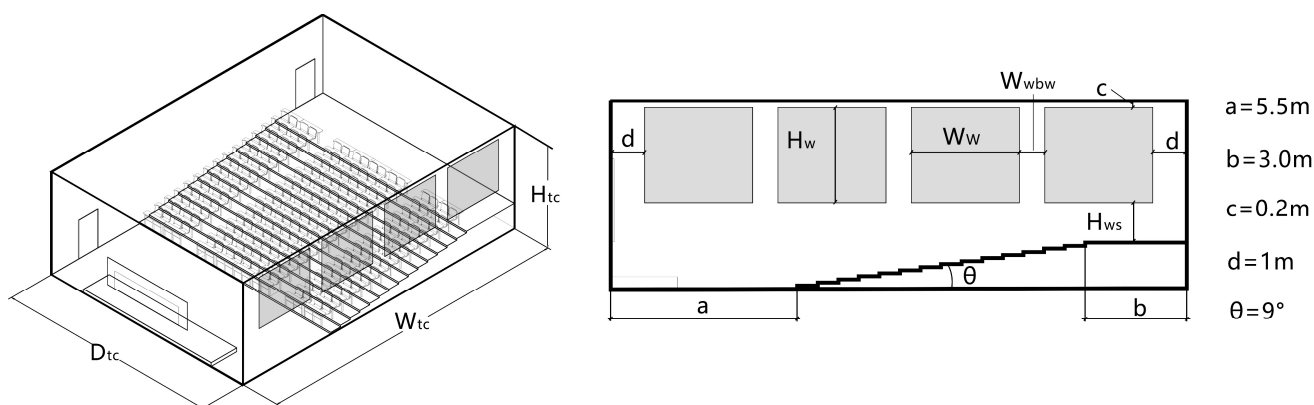


Figure 4. The geometric parameter information of simulation models.

This paper adopted the orthogonal experimental method [48] for the experimental design. Orthogonal experiment design is a scientific method for studying and dealing with multi-factor experiments. This method uses an orthogonal table to scientifically select the test conditions and reasonably carry out the multi-factor test by analyzing part of the test's results to master the overall test situation, and then optimize the optimal horizontal combination. According to the relevant regulations of terrace classrooms in the public teaching buildings of colleges and universities [46], the size of terrace classrooms was set as the common 150–360 students, and the corresponding room space varied from 16 to 23 m. The classroom depth varied from 12 to 15.5 m. According to the GB 50352–2019 standard [49], the windowsill height range was 0.6–1.3 m and the window height was 1.4–2.8 m. It is required in the GB 50352-2019 standard [47] that the width of the walls between windows should not be greater than 1.2 m, and when the width of the walls between windows is less than 1 m, constructional columns should be set. Therefore, the width range of the walls between windows was set to be 0–1.2 m, varying at unequal spacing. The number of walls between windows ranges from 1 to 8. The values of each factor and level are shown in Table 1. SPSS was used to generate orthogonal experiments [50], and 64 terrace classroom simulation models were formed. The experiment combined east, south, west, and north (four orientations) and finally determined 256 simulation models. The direction of the classroom in this paper refers to the orientation of the window wall.

Table 1. Design factors and levels of terrace classrooms.

Level	Classroom Width	Classroom Depth	Window Height	Windowsill Height	Width of Wall Between Windows	Number of Walls Between Windows
1	16 m	12 m	1.4 m	0.6 m	0 m	1
2	17 m	12.5 m	1.6 m	0.7 m	0.3 m	2
3	18 m	13 m	1.8 m	0.8 m	0.45 m	3
4	19 m	13.5 m	2 m	0.9 m	0.6 m	4
5	20 m	14 m	2.2 m	1 m	0.75 m	5
6	21 m	14.5 m	2.4 m	1.1 m	0.9 m	6
7	22 m	15 m	2.6 m	1.2 m	1.05 m	7
8	23 m	15.5 m	2.8 m	1.3 m	1.2 m	8

2.4.3. Initial Parameter Settings

1. Weather Data File and Material Properties

The US Department of Energy website's weather data file retrieved via Ladybug uses the Shenyang (123.25° E, 41.48°N) weather file by EnergyPlus [45].

According to the reflectance range described in GB50033-2013 [34], combined with Shenyang's geographical location and the terrace classroom's actual situation, the reflectance of the floor, wall, and ceiling was set as 0.30, 0.55, and 0.75, respectively. The interior windows comprised laminated glass with a visible light transmission ratio of 0.88.

2. Measuring Point Setup and Simulation Process

According to the GB/T 5699-2017 standard [51], the horizontal plane with a vertical height of 0.75 m from the ground was set as the illuminance calculation plane. According to the size of the interior space, the calculation plane was divided into analysis grids of 1.0 m × 1.0 m. The measuring points were located in the center of each grid, and the spacing between the measuring points was 1.0 m. The simulation time was set from 8:00 to 18:00 every day.

The meteorological data files, material parameters, analysis grid, and simulation time determined above were inputted into the designated positions in the program. The built-in daylight simulation engines, Ladybug and Honeybee, were run. The 256 models determined above were simulated and sorted into groups according to their orientation; finally, the data were obtained.

2.5. Statistical Analysis

This paper used statistical methods such as correlation analysis and multiple linear regression analysis to explore the influence of interior space and window geometry parameters on daylighting evaluation indicators in a terrace classroom. Firstly, a correlation analysis was conducted between independent variables (classroom interior space and window geometry) and dependent variables ($sDA_{300,50\%}$ and $UDI_{100-2000}$) to determine the degree and linear trend of linear correlations between each parameter and the evaluation index of the natural lighting environment. Pearson's correlation coefficient in SPSS was used to determine the existence of correlation and the closeness of the relationship between variables [52]. Next, multiple linear regression analysis [42,53], which has been used in several relevant studies, was selected to establish the prediction models of the terrace classrooms' interior space and window geometry parameters, and the $sDA_{300,50\%}$ and $UDI_{100-2000}$ in the terrace classroom facing each orientation, by using SPSS software.

3. Results

3.1. Correlation Analysis

This study conducted a linear correlation analysis between the interior space and window geometry of terrace classrooms facing east, south, west, and north using $sDA_{300,50\%}$ and $UDI_{100-2000}$. Table 2 shows the results of the correlation analysis. According to the definition of a significant correlation, when the significance value (Sig.) is less than 0.05, the independent and dependent variables are significantly correlated. In addition, the correlation coefficient (r) indicates the degree of closeness between the independent and dependent variables. The greater the absolute value of the correlation coefficient, the closer the relationship.

Table 2. Correlation analysis results of interior space and window geometry parameters with $sDA_{300,50\%}$ and $UDI_{100-2000}$.

Orientation	Index	W_{tc}	D_{tc}	H_{tc}	W_w	H_w	W_{wbw}	H_{ws}	N_w	WWR	WFR
East	SDA	0.331 **	-0.405 **	0.663 **	0.309 *	0.664 **	-0.232	0.156	-0.246	0.591 **	0.883 **
	UDI	0.415 **	-0.097	0.322 **	0.060	0.215	0.057	0.291 *	-0.057	0.159	0.230
South	SDA	0.309 *	-0.315 *	0.702 **	0.267 *	0.693 **	-0.208	0.183	-0.211	0.575 **	0.844 **
	UDI	0.273 *	0.022	-0.246 *	-0.119	-0.367 **	0.313 *	0.184	0.244	-0.381 **	-0.454 **
West	SDA	0.294 *	-0.328 **	0.693 **	0.254 *	0.694 **	-0.230	0.162	-0.203	0.583 **	0.858 **
	UDI	0.376 **	-0.084	0.042	-0.059	-0.098	0.266 *	0.292 *	0.067	-0.212	-0.163
North	SDA	0.329 **	-0.399 **	0.646 **	0.321 **	0.642 **	-0.245	0.159	-0.260 *	0.595 **	0.877 **
	UDI	0.412 **	-0.190	0.492 **	0.135	0.399 **	-0.031	0.301 *	-0.118	0.311 *	0.463 **

Notes: * and ** represent significant test results at 5% and 1% levels, respectively.

W_{tc} is positively correlated with $sDA_{300,50\%}$ and $UDI_{100-2000}$ for each classroom orientation, while other parameters have different linear correlations with $sDA_{300,50\%}$ and $UDI_{100-2000}$ for each classroom orientation. WFR, H_{tc} , H_w , WWR, W_{tc} , and W_w had a significant linear positive correlation with $sDA_{300,50\%}$ in the terrace classrooms facing each orientation, and the correlation degree decreased in turn. This indicates that the above parameters positively affect $sDA_{300,50\%}$, and the effect degree decreases successively. In addition, D_{tc} and $sDA_{300,50\%}$ for each classroom orientation had significant linear negative correlations, with an $|r|$ value between 0.315 and 0.405, which shows that the D_{tc} for the $sDA_{300,50\%}$ for each classroom orientation had certain inhibitions. In addition, N_w was only negatively correlated with $sDA_{300,50\%}$ in north-facing classrooms but to a low degree.

In addition, for east-facing classrooms, W_{tc} , H_{tc} , and H_{ws} were significantly positively correlated with $UDI_{100-2000}$, and the degree of correlation decreased successively. W_{tc} , H_{ws} , and W_{wbw} were positively correlated with $UDI_{100-2000}$, and their effects decreased successively for west-facing classrooms. WFR, WWR, H_w , and H_{tc} were negatively correlated with $UDI_{100-2000}$ in south-facing classrooms but positively correlated with $UDI_{100-2000}$ in north-facing classrooms. In addition, the correlation coefficients between $UDI_{100-2000}$

and each parameter for each orientation of the classroom were relatively small, with an $|r|$ value between 0.25 and 0.50.

3.2. Exploratory Analysis

The relationships between terrace classrooms' $sDA_{300,50\%}$ and $UDI_{100-2000}$ and geometry parameters that have significant influences on them were further analyzed by a boxplot. The lines in the box are the medians; the top and bottom edges of the box indicate the 75th and 25th percentile of all values sorted from the smallest to the largest, and the top and bottom T-bars indicate maximum and minimum values, respectively.

3.2.1. Interior Space Geometry Parameters and Daylighting Performance Evaluation Indices

In terms of the terrace classroom width, when W_{tc} was within the range of 16–19 m, with the increase in W_{tc} , the median value of $sDA_{300,50\%}$ of the terrace classrooms facing each orientation showed an obvious upward trend (Figure 5a), among which the south-facing classroom's $sDA_{300,50\%}$ increased the most. When W_{tc} increased from 19 m to 20 m, the median value of $sDA_{300,50\%}$ changed a little in terrace classrooms facing each orientation. When W_{tc} ranged from 20 to 23 m, the value of the terrace classrooms facing each orientation resumed an upward trend, among which the increase in the value of south-facing classrooms was the lowest. In addition, as W_{tc} gradually increased, the median $sDA_{300,50\%}$ was always the highest in south-facing classrooms, followed by west-facing classrooms, and it was similar and the lowest in east-facing and north-facing classrooms.

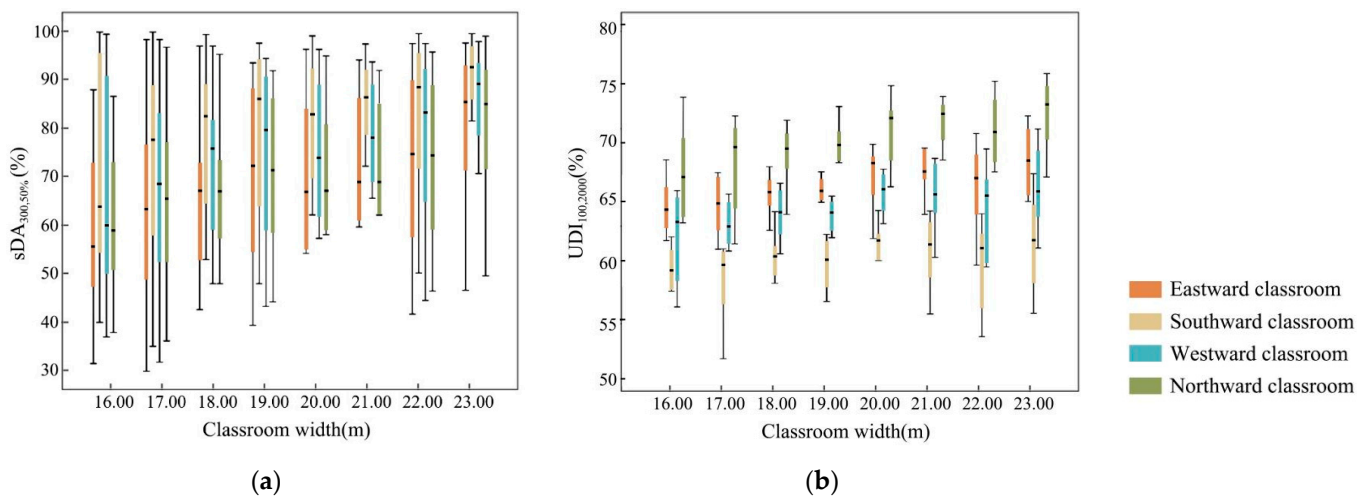


Figure 5. The analysis results of the distribution interval between the classroom width and the evaluation indices: (a) the analysis results of $sDA_{300,50\%}$; (b) the analysis results of $UDI_{100-2000}$.

When W_{tc} was 16–20 m, with the increase in W_{tc} , the median values of $UDI_{100-2000}$ in the terrace classrooms facing each orientation showed an upward trend (Figure 5b). When the W_{tc} was between 20 and 23 m, with the increase in W_{tc} , the median values of south and west $UDI_{100-2000}$ tended to be stable, while the median values of $UDI_{100-2000}$ in the east- and north-facing classrooms showed an upward trend. In addition, the median values of $UDI_{100-2000}$ in the north-, east-, west-, and south-facing classrooms decreased in turn.

In terms of the terrace classroom depth, with the increase in D_{tc} , the $sDA_{300,50\%}$ of the terrace classrooms facing each orientation showed an overall downward trend (Figure 6). When D_{tc} increased from 12.5 m to 13 m and from 14 m to 14.5 m, the median value of $sDA_{300,50\%}$ of the terrace classrooms facing each orientation decreased significantly. In addition, the median value of $sDA_{300,50\%}$ was the highest in south-facing classrooms, followed by west-facing classrooms. East-facing and north-facing classrooms exhibit similar sufficiency and the lowest daylight sufficiency.

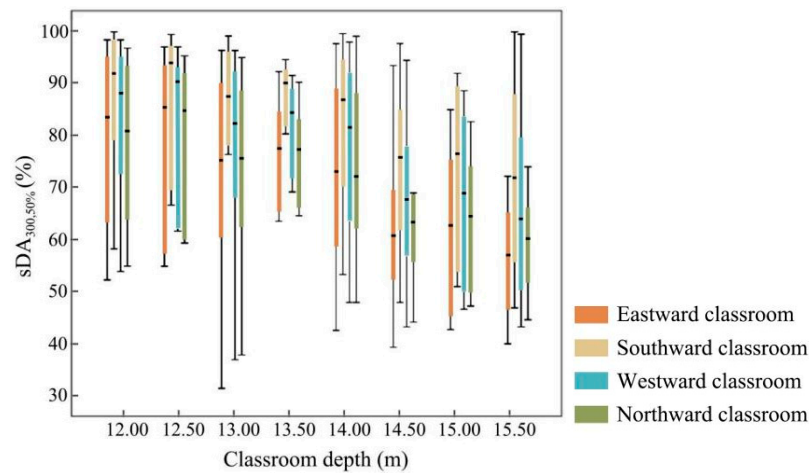


Figure 6. The analysis results of the distribution interval between the classroom depth and the evaluation index.

In terms of the terrace classroom height, when H_{tc} was within the range of 2.5–3.4 m, with the increase in H_{tc} , the median and interquartile values of $sDA_{300,50\%}$ of the terrace classrooms facing each orientation showed an obvious upward trend (Figure 7a). When H_{tc} increased from 3.4 m to 3.7 m, the median value of $sDA_{300,50\%}$ of the terrace classroom facing each orientation changed a little. When the H_{tc} was 3.7–4.3 m, the median value of $sDA_{300,50\%}$ showed a slight upward trend. In addition, when the H_{tc} was 2.5–2.8 m, the median $sDA_{300,50\%}$ of west-facing and north-facing classrooms was similar and about 5% higher than that of east-facing classrooms. When the H_{tc} was 3.1–4.3 m, the median $sDA_{300,50\%}$ of the east- and north-facing classrooms was similar and lower than that of the east-facing classroom. The median $sDA_{300,50\%}$ was always the highest in the south-facing classroom.

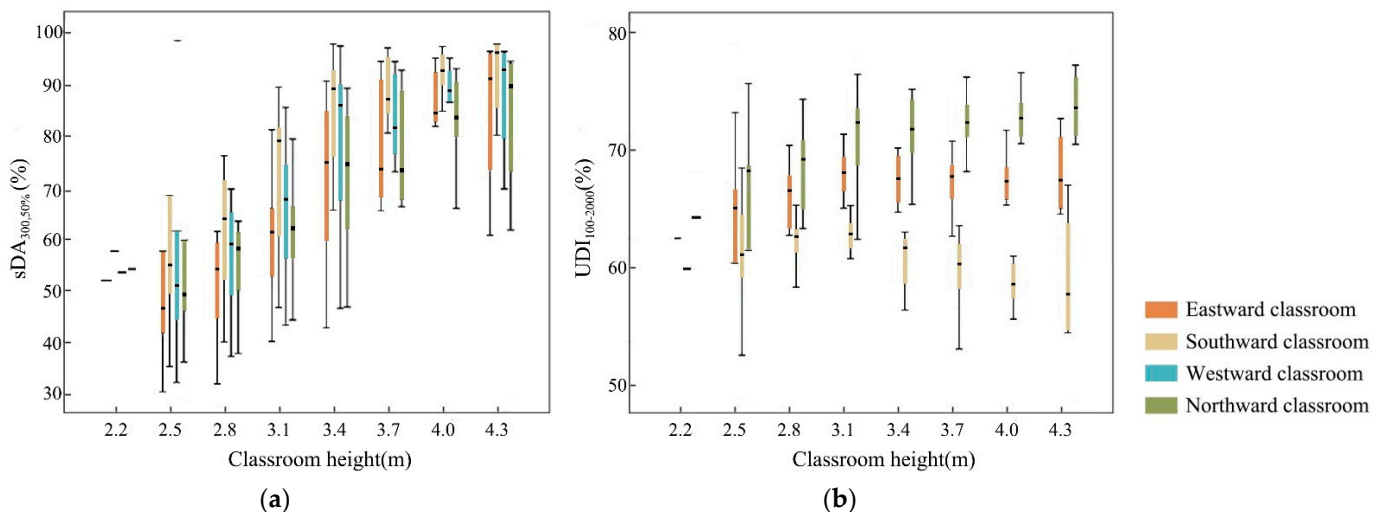


Figure 7. The analysis results of the distribution interval between the classroom height and the evaluation indices: (a) the analysis results of $sDA_{300,50\%}$; (b) the analysis results of $UDI_{100-2000}$.

When H_{tc} was within the range of 2.2–3.1 m, with the increase in H_{tc} , the median value of $UDI_{100-2000}$ in east-, south-, and north-facing terrace classrooms showed an obvious upward trend (Figure 7b). With the increase in H_{tc} in the range of 3.1–4.3 m, the changing trend of $UDI_{100-2000}$ was different for the terrace classrooms facing each orientation, among which the median values of $UDI_{100-2000}$ in south-facing, east-facing, and north-facing classrooms decreased, stabilized, and slightly increased, respectively.

3.2.2. Window Geometry Parameters and Daylighting Performance Evaluation Indices

In terms of the window width, when W_w was 0.5–4.1 m, the median value of the $sDA_{300,50\%}$ of the terrace classrooms facing each orientation showed a slight upward trend with the increase in W_w (Figure 8). When W_w increased from 4.1 m to 5.3 m, the median value of the $sDA_{300,50\%}$ of the terrace classrooms facing each orientation decreased slightly. When W_w was 5.3–8.9 m, the $sDA_{300,50\%}$ of the terrace classrooms facing each orientation resumed a slight upward trend. In addition, the median value of $sDA_{300,50\%}$ in south-facing classrooms was the highest, followed by west-facing classrooms. East-facing and north-facing classrooms exhibited similar sufficiency and the lowest daylight sufficiency.

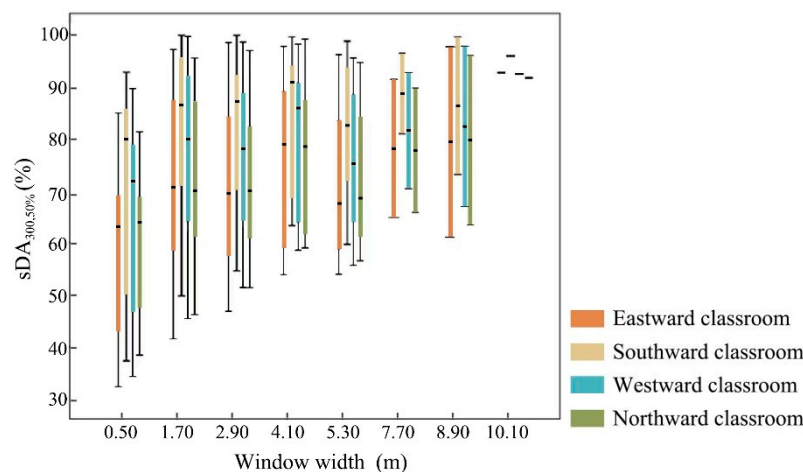


Figure 8. The analysis results of the distribution interval between the window width and the evaluation index.

In terms of the window height, as H_w increased from 1.4 m to 2.4 m, the $sDA_{300,50\%}$ of the terrace classrooms facing each orientation showed a significant increasing trend (Figure 9a). When H_w was within 1.4–2.4 m, the median $sDA_{300,50\%}$ of east-facing and north-facing classrooms was close. The difference between them and the median $sDA_{300,50\%}$ of west-facing and south-facing classrooms gradually increased with an increase in H_w . In addition, the median value of $sDA_{300,50\%}$ in south-facing classrooms was always the highest. When H_w increased within 2.4–2.8 m, the $sDA_{300,50\%}$ tended to be stable in the terrace classrooms facing each orientation, with the median and interquartile range values of $sDA_{300,50\%}$ being higher in south-facing classrooms, moderate in west-facing classrooms, and similar and lowest in east-facing and north-facing classrooms, respectively.

Additionally, for south-facing terrace classrooms, the median values of $UDI_{100-2000}$ tended to be stable when H_w was within the range of 1.4–1.8 m (Figure 9b). Moreover, the median values of $UDI_{100-2000}$ showed a slightly decreasing trend as H_w gradually increased from 1.8 m to 2.8 m. For north-facing terrace classrooms, the median $UDI_{100-2000}$ showed an apparent upward trend when H_w increased in 1.4–2.0 m, after which the $UDI_{100-2000}$ median values leveled off as H_w continued increasing. Furthermore, the median value of the $UDI_{100-2000}$ of north-facing classrooms was always larger than those of south-facing classrooms, with a maximum difference of about 15%.

In terms of the width of the wall between windows, with the gradual increase in W_{wbw} within the range of 0–0.9 m, the $UDI_{100-2000}$ of south-facing and west-facing terrace classrooms showed an upward trend (Figure 10). After that, as W_{wbw} continued increasing, the median value of $UDI_{100-2000}$ in south-facing and west-facing classrooms decreased and changed significantly. In addition, the $UDI_{100-2000}$ of the west-facing classrooms was consistently larger than that of the south-facing classrooms, with a maximum difference of about 5%.

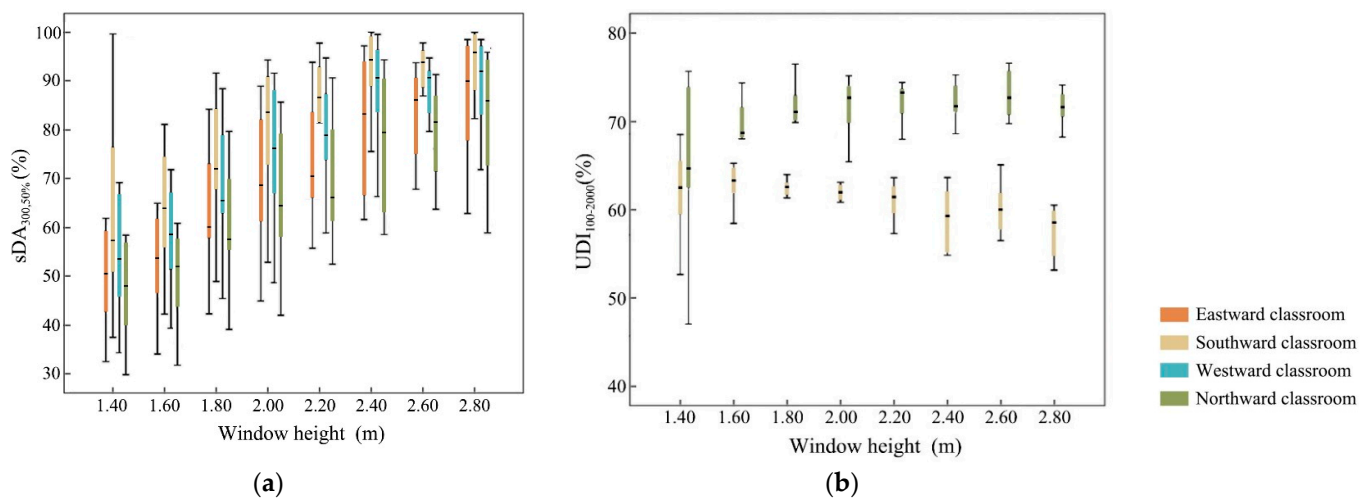


Figure 9. The analysis results of the distribution interval between the window height and the evaluation indices: (a) the analysis results of $sDA_{300,50\%}$; (b) the analysis results of $UDI_{100-2000}$.

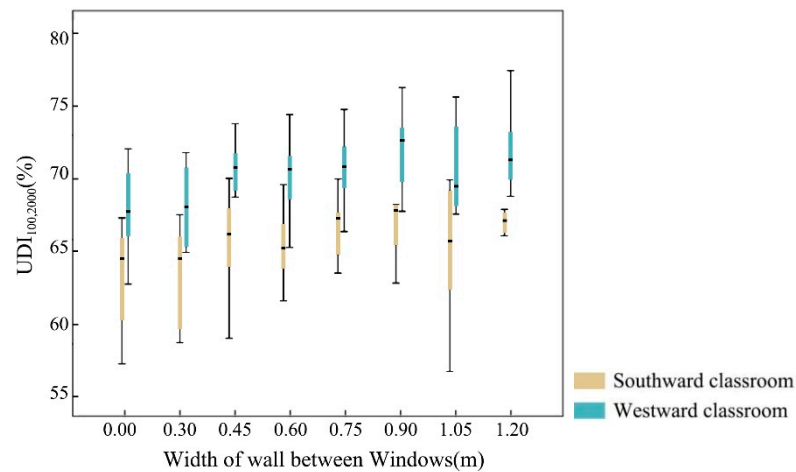


Figure 10. The analysis results of the distribution interval between the width of the wall between windows and the evaluation index.

In terms of the windowsill height, the median values of $UDI_{100-2000}$ for north-facing classrooms showed an increasing trend as H_{ws} increased (Figure 11). Moreover, as H_{ws} gradually increased in the range of 0.6–1.0 m, the median values of $UDI_{100-2000}$ for east-facing and west-facing classrooms showed a steady and slightly decreasing trend, respectively. With the gradual increase in H_{ws} in 1.0–1.3 m, the median $UDI_{100-2000}$ value in east-facing and west-facing classrooms showed an upward trend. In addition, the median value of $UDI_{100-2000}$ in north-facing, east-facing, and west-facing classrooms decreased sequentially.

In terms of the number of windows, only N_w in north-facing classrooms had a significant impact on $sDA_{300,50\%}$ (Figure 12). When N_w was 4, the median value of $sDA_{300,50\%}$ was about 15% higher than other N_w . When N_w was 5–9, with the increase in N_w , the median value of $sDA_{300,50\%}$ changed a little, while the maximum and minimum values showed a clear downward trend.

In terms of the window–wall ratio, with the increase in WWR, the $sDA_{300,50\%}$ of the terrace classrooms facing each orientation showed an upward trend, and the median value of $sDA_{300,50\%}$ in south-facing classrooms was always the highest (Figure 13a). Among them, when the WWR was 0.20–0.30, the $sDA_{300,50\%}$ of west-facing and north-facing classrooms was similar, and the median value was greater than that of east-facing classrooms by about 5%. When the WWR was in the range of 0.30–0.60, the $sDA_{300,50\%}$ of east-facing and north-facing classrooms was similar, with median values that were about 10% and 17% smaller than those in west-facing and south-facing classrooms, respectively. When the WWR was

0.60–0.70, the median $sDA_{300,50\%}$ in east-, west-, and north-facing classrooms was similar and about 5% smaller than in the south.

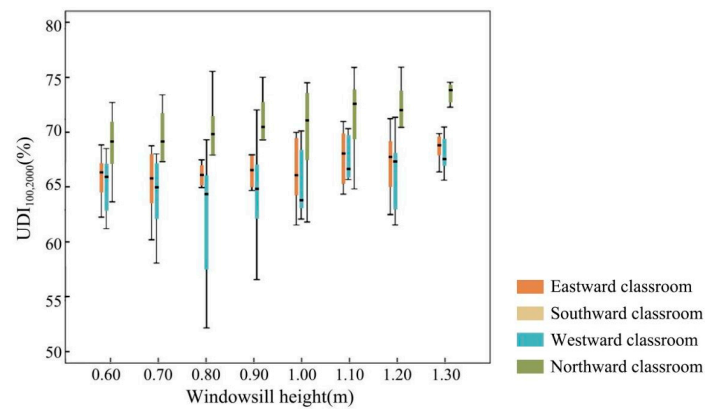


Figure 11. The analysis results of the distribution interval between the windowsill height and the evaluation index.

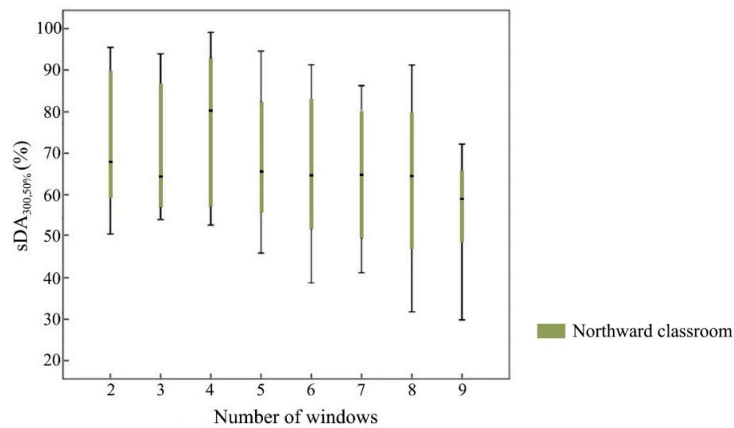


Figure 12. The analysis results of the distribution interval between the number of windows and the evaluation index.

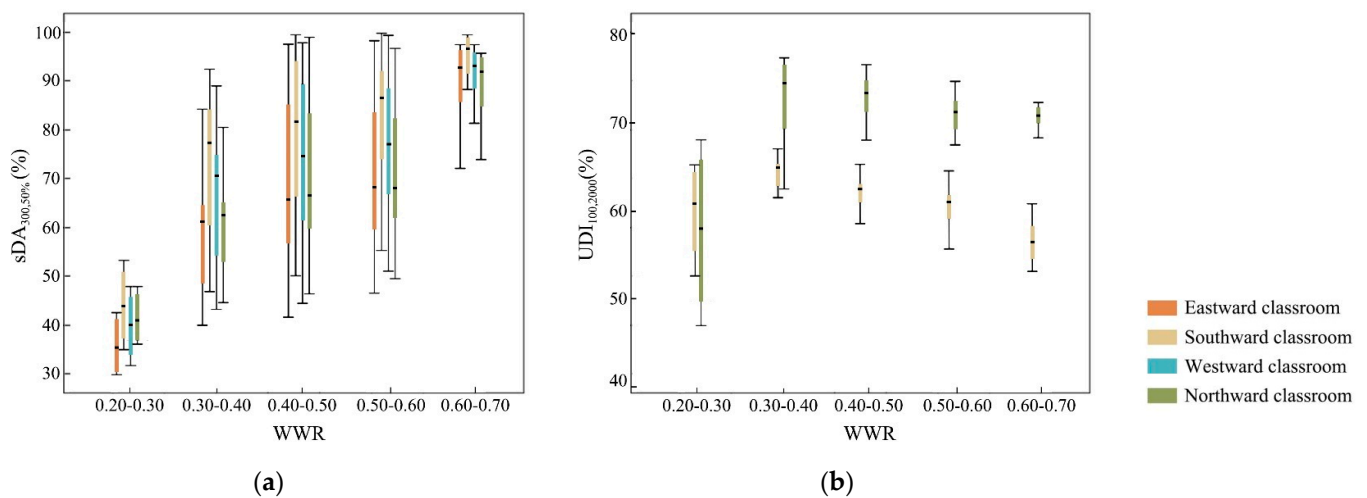


Figure 13. The analysis results of the distribution interval between WWR and the evaluation indices: (a) the analysis results of $sDA_{300,50\%}$; (b) the analysis results of $UDI_{100-2000}$.

For south-facing and north-facing terrace classrooms, when the WWR increased from 0.2–0.3 to 0.3–0.4, $UDI_{100-2000}$ showed a clear upward trend, and the increase in north-facing classrooms was significantly larger (Figure 13b). As the WWR gradually increased in the

range of 0.3–0.7, the $UDI_{100-2000}$ of the two classrooms showed a downward trend, and the median value of $UDI_{100-2000}$ in the north-facing classroom was about 10% greater than that of the south.

In terms of the window–floor ratio, with the increase in WFR, the $sDA_{300,50\%}$ of the terrace classrooms facing each orientation showed a clear upward trend, and the median value of $sDA_{300,50\%}$ in the south-facing classroom was always the highest (Figure 14a). When the WFR was within the range of 0.04–0.11, the median $sDA_{300,50\%}$ value of west- and north-facing classrooms was similar and about 4% greater than that of east-facing classrooms. When the WFR was in the range of 0.11–0.17, the $sDA_{300,50\%}$ of east-facing and north-facing classrooms was similar, and the median value was lower than that of west-facing classrooms by about 5–10%. When the WFR was 0.17–0.20, the median $sDA_{300,50\%}$ value difference between classrooms was small.

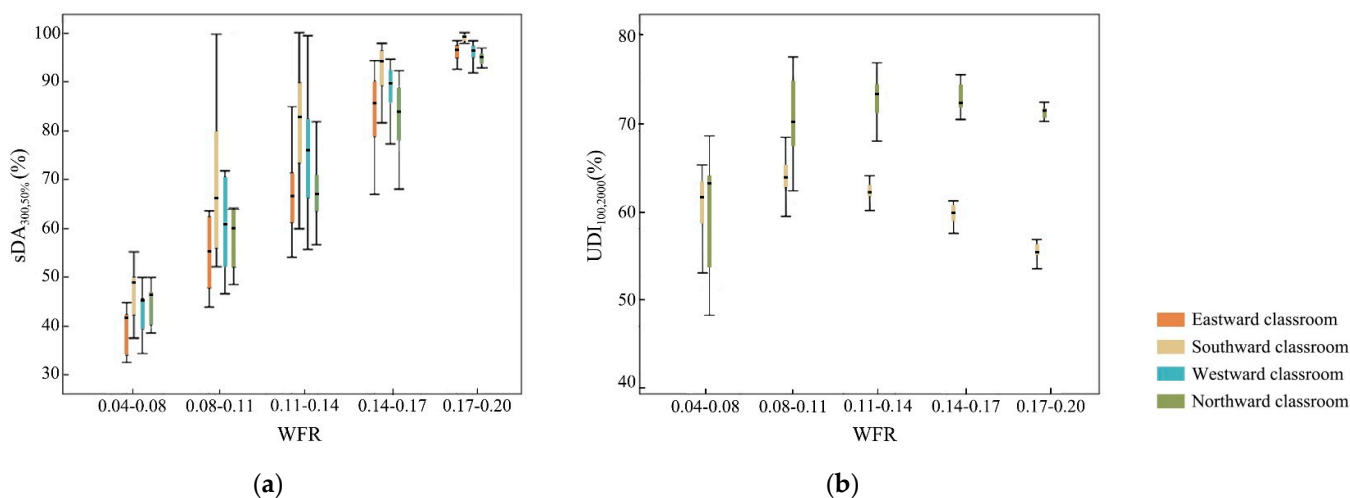


Figure 14. The analysis results of the distribution interval between WFR and the evaluation indices: (a) the analysis results of $sDA_{300,50\%}$; (b) the analysis results of $UDI_{100-2000}$.

As the WFR gradually increased within the range of 0.04–0.11, the median value of $UDI_{100-2000}$ in the south-facing terrace classrooms showed an upward trend. Later, as the WFR continued to increase, $UDI_{100-2000}$ showed a clear downward trend (Figure 14b). When the WFR gradually increased in the range of 0.04–0.14, the median $UDI_{100-2000}$ value in north-facing classrooms showed an upward trend; then, $UDI_{100-2000}$ decreased slightly as the WFR continued to increase. In addition, the $UDI_{100-2000}$ in the north-facing classroom was always larger than in the south-facing classroom, and the maximum difference between the two-facing $UDI_{100-2000}$ was about 15%.

3.3. Prediction Model

According to the correlation analysis results of the interior space geometry parameters and window geometry parameters of terrace classrooms with $sDA_{300,50\%}$ and $UDI_{100-2000}$, the geometry parameters with a significant influence on $sDA_{300,50\%}$ and $UDI_{100-2000}$ were taken as independent variables, and $sDA_{300,50\%}$ and $UDI_{100-2000}$ were taken as dependent variables for the multiple linear regression analysis. Prediction models for the $sDA_{300,50\%}$ and $UDI_{100-2000}$ of terrace classrooms facing each orientation were constructed.

Firstly, to describe the quantitative relationship between variables more accurately, the curve estimation method was used to fit the selected geometrical parameters (independent variables) with $sDA_{300,50\%}$ and $UDI_{100-2000}$ (dependent variables) with various curve types, and based on the significance index (Sig.) values, to determine the curve relationship between variables. This study focuses on several common curve models, including linear, conic, cubic, and logarithmic curve models.

To comprehensively consider the interactive effects of geometry parameters in the regression model and seek the optimal combination of geometry parameters that can explain

the variation law of differently oriented terrace classrooms' $sDA_{300,50\%}$ and $UDI_{100-2000}$, in this study, the curve fitting model exhibiting statistical significance between each geometrical parameter, and terrace classroom's $sDA_{300,50\%}$ and $UDI_{100-2000}$, were selected as independent variables and comprehensively applied to the regression analysis. Using multiple linear regression step-by-step methods, multiple iterative regression analyses for different variable combinations were carried out. Finally, the optimal variable combination was selected, and the prediction model was built.

The regression equation for the $sDA_{300,50\%}$ (%) of the terrace classrooms facing each orientation is as follows.

$$sDA_{300,50\%}(\text{eastward}) = 0.002 \cdot W_{tc}^3 - 103.920 \cdot WWR^3 + 613.203 \cdot WFR + 0.256, \quad (1)$$

$$sDA_{300,50\%}(\text{southward}) = 0.001 \cdot W_{tc}^3 - 78.776 \cdot WWR^2 + 60.087 \cdot \ln(WFR) + 223.122, \quad (2)$$

$$sDA_{300,50\%}(\text{westward}) = 0.001 \cdot W_{tc}^3 - 75.377 \cdot WWR + 63.075 \cdot \ln(WFR) + 242.057, \quad (3)$$

$$sDA_{300,50\%}(\text{northward}) = 0.002 \cdot W_{tc}^3 - 114.202 \cdot WWR^3 + 693.732 \cdot WFR - 12.771 \cdot \ln(H_w) - 0.945, \quad (4)$$

The adjusted R^2 of the multiple linear regression model for east-, south-, west-, and north-facing classrooms' $sDA_{300,50\%}$ is 0.885, 0.861, 0.844, and 0.882, respectively, indicating that the interpretation degree of the model for the east-, south-, west-, and north-facing classrooms' $UDI_{100-2000}$ is 88.5%, 86.1%, 84.4%, and 88.2%, respectively. The model has high goodness of fit. The significant values (Sig.) of the regression models in the variance analyses were all lower than 0.05, indicating that the established regression models had significant statistical significance. The Sig. values in the t-test were all less than 0.05, indicating that the regression coefficients were significant, and there was a significant correlation between the independent and dependent variables. In addition, the variance inflation factors (VIF) of the independent variables ranged from 1.029 to 5.622, all of which were lower than 10, indicating no multicollinearity in the models (Table 3).

Table 3. Comprehensive analysis results of multiple regression models of $sDA_{300,50\%}$ in differently orientated terrace classrooms.

Orientation	Adjusted R^2	Sig.	Independent Variable	Standardized Coefficients	t	Sig.	VIF
East	0.885	0.000	Constant	—	0.073	0.042	—
			W_{tc}^3	0.260	6.000	0.000	2.442
			WWR^3	−0.383	−5.687	0.000	1.029
			WFR	1.147	17.158	0.000	2.479
South	0.861	0.000	Constant	—	19.317	0.000	—
			W_{tc}^3	0.207	4.338	0.000	1.032
			WWR^2	−0.427	−5.624	0.000	2.619
			$\ln(WFR)$	1.180	15.611	0.000	2.594
West	0.844	0.000	Constant	—	14.630	0.000	—
			W_{tc}^3	0.200	3.947	0.000	1.037
			WWR	−0.434	−4.996	0.000	3.054
			$\ln(WFR)$	1.198	13.895	0.000	3.010
North	0.882	0.000	Constant	—	−0.254	0.008	—
			W_{tc}^3	0.249	5.467	0.000	1.038
			WWR^3	−0.420	−5.496	0.000	2.921
			WFR	1.294	12.214	0.000	5.622
			$\ln(H_w)$	−0.162	−2.177	0.034	2.791

In addition, according to the standardized regression coefficient, the influence of WFR, WWR^2 , and W_{tc}^3 on the $sDA_{300,50\%}$ in the east-facing and north-facing classrooms decreased successively. For the north-facing classrooms, $\ln(H_w)$ was only more influential

than W_{tc}^3 . For the $sDA_{300,50\%}$ prediction model for south- and west-facing classrooms, WWR^2 and WWR had the greatest influence, followed by W_{tc}^3 , and $\ln(WFR)$ had the least influence.

The regression equation for the $UDI_{100-2000}$ (%) of the terrace classrooms facing each orientation is as follows.

$$UDI_{100-2000}(\text{eastward}) = 0.68 \cdot W_{tc} - 0.96 \cdot H_w^2 + 18.13 \cdot \ln(H_{tc}) + 37.01, \quad (5)$$

$$UDI_{100-2000}(\text{southward}) = -1670.36 \cdot WFR^3 + 12.45 \cdot \ln(W_{tc}) + 26.83, \quad (6)$$

$$UDI_{100-2000}(\text{westward}) = 13.98 \cdot \ln(W_{tc}) + 2.13 \cdot H_{ws}^3 + 3.08 \cdot W_{wbw} + 19.40, \quad (7)$$

$$UDI_{100-2000}(\text{northward}) = 15.00 \cdot \ln(W_{tc}) - 65.73 \cdot WWR^3 + 21.41 \cdot \ln(WFR) - 0.21 \cdot H_w^3 + 84.07, \quad (8)$$

The adjusted R^2 of the multiple linear regression model for east-, south-, west-, and north-facing classrooms' $UDI_{100-2000}$ is 0.310, 0.385, 0.287, and 0.774, respectively, indicating that the interpretation degree of the model for the east-, south-, west-, and north-facing classrooms' $UDI_{100-2000}$ is 31%, 38.5%, 28.7%, and 77.4%, respectively. The model has high goodness of fit. The significant values (Sig.) of the regression models in variance analyses were all less than 0.05, indicating that the established regression models had significant statistical significance. The Sig. values in the t-test were all less than 0.05, indicating that the regression coefficients were significant and there was a significant correlation between the independent and dependent variables. In addition, the variance inflation factor (VIF) of the independent variable ranged from 1.000 to 4.451, all of which are less than 10, indicating no multicollinearity in the models (Table 4).

Table 4. Comprehensive analysis results of multiple regression models of $UDI_{100-2000}$ in differently-orientated terrace classrooms.

Orientation	Adjusted R^2	Sig.	Independent Variable	Standardized Coefficients	t	Sig.	VIF
East	0.310	0.000	Constant	—	6.683	0.000	—
			W_{tc}	0.415	3.963	0.000	1.000
			H_w^2	-0.490	-2.221	0.030	4.451
			$\ln(H_{tc})$	0.773	3.501	0.001	4.451
South	0.385	0.000	Constant	—	2.475	0.016	—
			WFR^3	-0.574	-5.779	0.000	1.010
			$\ln(W_{tc})$	0.337	3.393	0.001	1.010
West	0.287	0.015	Constant	—	1.675	0.009	—
			$\ln(W_{tc})$	0.382	3.595	0.001	1.000
			H_{ws}^3	0.322	3.024	0.004	1.000
			W_{wbw}	0.266	2.504	0.015	1.000
North	0.774	0.000	Constant	—	8.215	0.000	—
			$\ln(W_{tc})$	0.349	5.496	0.000	1.056
			WWR^3	-0.842	-8.784	0.000	2.400
			$\ln(WFR)$	1.360	11.083	0.000	3.929
			H_w^3	-0.260	-2.916	0.005	2.081

In addition, according to the standardized regression coefficient, $\ln(H_{tc})$, H_w^2 , and W_{tc} successively reduced the influence on the $UDI_{100-2000}$ of the east-facing classrooms. For south-facing classrooms, WFR^3 had a greater influence on $UDI_{100-2000}$ than $\ln(W_{tc})$. For west-facing classrooms' $UDI_{100-2000}$, the influence of $\ln(W_{tc})$, H_{ws}^3 , and W_{wbw} gradually decreased. $\ln(WFR)$ had the greatest influence on the north-facing classrooms' $UDI_{100-2000}$, followed by WWR^3 and $\ln(W_{tc})$, and H_w^3 exhibited the least influence.

4. Discussion

4.1. Impact of Interior Space Geometry

H_{tc} , D_{tc} , and W_{tc} are three essential parameters affecting interior space. The correlation analysis showed a significant positive correlation between the H_{tc} and the $sDA_{300,50\%}$ of the terrace classrooms facing each orientation. With the increase in H_{tc} , the increasing range of $sDA_{300,50\%}$ of the classrooms facing each orientation gradually decreased. This is because daylight illuminance increased with H_{tc} , which led to the improvement of overall illuminance levels and an increase in the effective natural light area. When H_{tc} increased to 3.7 m, most interior areas reached the standard of $sDA_{300,50\%}$. After that, the increasing speed of the available lighting area in the terrace classrooms slowed down. Moreover, the results showed that the $UDI_{100-2000}$ of the east-facing, south-facing, and north-facing terrace classrooms had an apparent upward trend when H_{tc} increased gradually within the 2.2–3.1 m range. Later, with the increase in H_{tc} , the $UDI_{100-2000}$ of south-, east-, and north-facing classrooms showed a noticeable decline, a steady trend, and a slight increase, respectively. This is because the direct sunlight received by classrooms in the south, east, and north orientations decreased in turn. Therefore, when H_{tc} was low, with the increase in H_{tc} , the increasing gains in the amount of light entering mainly extended the time period of when illuminance exceeded the lower limit of $UDI_{100-2000}$, thus increasing the cumulative time of available illuminance for natural lighting. However, when H_{tc} continued increasing, the increase in the amount of light entering gradually extended the time period within which the south-facing classroom exceeded the upper limit illuminance of $UDI_{100-2000}$, resulting in a decrease in the cumulative time of available illuminance for natural lighting. In the east-facing terrace classrooms, the time exceeding the lower and upper limits of $UDI_{100-2000}$ illuminance increased with the continuous gain of daylighting, so the cumulative time of available illuminance for natural lighting tended to be stable. The increase in the amount of light entering for the north-facing classroom mainly extended the time period within which the lower limit illuminance of $UDI_{100-2000}$ was exceeded, thus continuing to increase the cumulative time of available illuminance for natural lighting.

With the increase in W_{tc} , the $sDA_{300,50\%}$ of the classrooms facing each orientation showed an upward trend. $UDI_{100-2000}$ in east- and north-facing classrooms continued to increase, while $UDI_{100-2000}$ in west- and south-facing classrooms increased and tended to be stable. During the construction of the simulation model, W_{tc} largely determined the range of W_w . When W_w increased, the increase in incoming daylight would increase the overall illuminance level and the available lighting area. Additionally, with the increase in W_{tc} within 16–20 m, the illuminance time below the lower limit of $UDI_{100-2000}$ gradually decreased, so $UDI_{100-2000}$ showed an upward trend. Later, with the further increase in W_{tc} , the cumulative time of available illuminance for natural lighting in east- and north-facing classrooms continued to increase. However, the amount of direct sunlight received in south- and west-facing classrooms amounts to more than that in east- and north-facing classrooms. With the further increase in W_{tc} , the time period in which the lower limit of $UDI_{100-2000}$ at the far window was exceeded increased continuously. In contrast, the time period in which the upper limit of $UDI_{100-2000}$ at the close window was exceeded increased gradually. Thus, the cumulative time of available illuminance for natural lighting tended to be stable.

Compared with W_{tc} , D_{tc} had a more significant impact on $sDA_{300,50\%}$ and negatively influenced the $sDA_{300,50\%}$ of the terrace classrooms facing each orientation. Voll et al. concluded that when the room was shallower and windows were larger, daylighting was better, which indicated that classroom depth was negatively correlated with $sDA_{300,50\%}$. This is the same as the result obtained in this paper [54]. Susorova et al. chose the ratio of room width to depth as one of the design parameters when studying the daylighting performance and energy consumption level of commercial office buildings. It was observed that classroom width determines the amount of received daylight, and classroom depth determines the distance of daylight penetration. Wide and shallow rooms have better daylighting performance. The increase in classroom depth will decrease the available lighting area, resulting in a significant increase in energy consumption [8]. Although the

use function and spatial form of research objects in this paper have differences, the research results are consistent with those of our predecessors. Therefore, attention should be focused upon the proportional relationship between D_{tc} and W_{tc} under different orientations and the choice of H_{tc} when designing the interior space of terrace classrooms.

Different orientations of the terrace classrooms have a great impact on daylighting performance. The results of the correlation analysis showed that in most cases, the interior space and window geometry parameters except D_{tc} were positively correlated with $sDA_{300,50\%}$ and $UDI_{100-2000}$ in east-, west-, and north-facing classrooms. However, due to the large amount of direct daylight received by south-facing terrace classrooms, H_w , H_{tc} , WWR , and WFR were significantly negatively correlated with the $UDI_{100-2000}$ of south-facing classrooms. In addition, due to the difference in the amount of light entering relative to differently oriented terrace classrooms, the south-facing classrooms performed best in $sDA_{300,50\%}$, followed by west-facing, and east- and north-facing classrooms performed worst. Ignacio Acosta et al. found that when the windows' geometries remained unchanged, the $DA_{250\text{ lx}}$ of the south-facing room was three times that of the north-facing room, and the $DA_{250\text{ lx}}$ of the east-facing or west-facing room was nearly twice that of the north-facing room [18]. Due to the differences between the study's site and object, the results of their analysis are different from this paper's numerical values. Nevertheless, the research results of the overall natural illuminance level of classrooms with different orientations in this paper again confirmed the above conclusions.

4.2. Impact of Window Geometry

H_w , W_w , H_{ws} , W_{wbw} , and N_w are the five important parameters that determine the geometry of windows. Among them, W_w and H_w determine the area of the individual windows. H_{ws} , W_{wbw} , and N_w determine the distribution of windows on the exterior wall.

Different H_w and W_w will have a great impact on daylighting performance. As H_w increased, the $sDA_{300,50\%}$ of the terrace classrooms facing each orientation first increased and then stabilized. $UDI_{100-2000}$ in south-facing classrooms first stabilized and then decreased, while the north-facing $UDI_{100-2000}$ and the south-facing $UDI_{100-2000}$ changed in reverse. Direct sunlight is the main source of indoor daylighting [55]. The higher the H_w , the less direct sunlight is blocked, and the higher the natural light illuminance level. When the amount of light entering reaches a certain level, almost all measurement points receive natural light above 300 lx all year round, and the time reaches 50%. At this moment, increasing H_w will not help the natural light illuminance levels much, and it will also increase the energy consumption of heating and cooling. Since the south-facing classroom can receive significantly more direct sunlight than the north-facing classroom, as the amount of light entering increased, the time for exceeding the upper limit illuminance of $UDI_{100-2000}$ in the south-facing classroom increased gradually. In contrast, the time below the lower limit illuminance of $UDI_{100-2000}$ in the north-facing classroom gradually decreased. Therefore, the north-facing classroom and the south-facing classroom changed in reverse. In addition, W_w is only positively correlated with $sDA_{300,50\%}$, and compared with H_w , W_w has less influence on daylighting performances. Deng et al. found that the increase in window height caused $sDA_{150,50\%}$ or $sDA_{450,50\%}$ to increase significantly more than the effect of a window's width on it in the daylighting performance of the reading room [56]. Although their research objects and study areas differed from this paper's, the results were consistent. In order to improve the quality of natural light, H_w and W_w should not be too large. Rupp et al. stated in their paper that while an increase in window area can increase lighting, controlling a certain window area can improve daylight availability [57]. Zheng simulated a total of seven groups of classrooms facing 0–30° southeast and concluded that $UDI_{100-2000}$ decreased with an increase in window height, which is consistent with the local curve trend of south-facing classrooms in this paper [58]. After simulating the influence of north–south facing classroom window height on the natural light environment, Zhang pointed out that for south-facing classrooms, choosing a larger window height size can improve the daylighting quality of the classroom, which is inconsistent with the results of this paper [59];

this is because her research subjects were ordinary classrooms with interior spaces and window geometry that were quite different from those in this study.

The results of the correlation analysis showed that the south- and west-facing terrace classrooms' $UDI_{100-2000}$ are positively correlated with W_{wbw} . Deng et al. confirmed that the enlargement of the width of the wall between windows could improve the illuminance uniformity of the deeper areas of the room while introducing a certain shading effect [56]. In addition, this paper's results showed a significant positive correlation between $UDI_{100-2000}$ and H_{ws} in east-, west-, and north-facing classrooms. With the increase in H_{ws} , the north-facing classrooms' $UDI_{100-2000}$ always reflected an upward trend, and the east- and west-facing classrooms' $UDI_{100-2000}$ reflected a downward and then upward trend. For east- and west-facing classrooms, when H_{ws} was less than 0.75 m of the working plane's height, as H_{ws} increased, direct sunlight near the window increased, and the $UDI_{100-2000}$ in the classroom decreased; when H_{ws} was greater than 0.75 m, as H_{ws} increased, the light reaching the depth of the classroom increased, while direct light near the window decreased, and the $UDI_{100-2000}$ in the classroom increased. Since there was no direct light in the north-facing classroom, the $UDI_{100-2000}$ always increased as H_{ws} increased. Allam et al. mentioned in their analysis of the relationship between windowsill height and lighting energy that when the windowsill's height is higher, the amount of blocked direct sunlight increases. That is, the natural light illuminance level will decrease with the increase in windowsill height, and sDA will decrease [55]. Therefore, in architectural designs, the relationship between the time period between the available illuminance for natural lighting and the illuminance adequacy of natural light should be balanced, and an appropriate H_{ws} should be used.

For WWR and WFR, as WWR or WFR increased, the $sDA_{300,50\%}$ of the terrace classrooms facing each orientation showed a clear upward trend. Both the south-facing and north-facing classrooms' $UDI_{100-2000}$ showed increasing and then decreasing trends, but the decreasing trend of north-facing classrooms was smaller than that of south-facing classrooms. Since the south-facing classroom can receive more direct sunlight than the north-facing classroom, and when the WWR or WFR is small, with the increase in WWR or WFR, the increase in the amount of light entering mainly increases the time period in which the south- and north-facing classrooms exceed the lower limit illuminance of $UDI_{100-2000}$, thereby increasing the cumulative time of available illuminance for natural lighting. However, when WWR and WFR increased to a certain extent, as the amount of light entering continued to grow, the excess direct sunlight in the south-facing classroom led to a significant increase in the time period within which illuminance exceeded the upper limit of $UDI_{100-2000}$; thus, the cumulative time of available illuminance for natural lighting decreased significantly. The intensity of sunlight incidence in the north-facing classroom is relatively low, so the decrease in $UDI_{100-2000}$ is relatively small. Fila et al. pointed out in their study that when WWR reached 10%, the overall illuminance level significantly improved. When WWR increases to 30% or even 50%, the room will contain too much sunlight, which will increase the time period within which the upper limit illuminance of $UDI_{100-2000}$ is exceeded, which is not conducive for the improvement of daylighting performance [60]. The change trend of $UDI_{100-2000}$ obtained from the above studies is basically consistent with that in this paper, but because the research site is located in a low-latitude tropical region and the research object is located in mid-latitude temperate zones, there are great differences in the variation intervals of WWR.

4.3. Limitation

The study site of this paper was in Shenyang, so applying results to regions with different climates or latitudes than Shenyang is difficult. In addition, this paper only analyzes the most common unilateral natural lighting conditions in the terrace classrooms of universities in severe cold regions, and the classroom's size is set to the most common 150~360 people. Moreover, considering the need for the overall effect of the facade in

architectural designs, the windows are only evenly arranged horizontally. Therefore, comparing the study's results with studies in different settings is difficult.

Various scales of terrace classrooms and window arrangements in different climate zones will be studied in the future. In addition, glare and reflection problems in the classroom and other indoor physical environment variables will be combined to conduct a comprehensive study to effectively improve the quality of the indoor environment.

5. Conclusions

This paper used Shenyang as an example. The relationship between interior spaces and window geometries and the daylighting performance of university terrace classrooms in severe cold areas was studied by combining numerical simulations and statistical analyses, which provided a quantitative reference and evaluation basis for designing university terrace classrooms. The findings and design recommendations are as follows:

1. WFR, H_{tc} , H_w , WWR, W_{tc} , and W_w positively affected the $sDA_{300,50\%}$ of the terrace classrooms facing each orientation, and the degree of effect decreased sequentially. D_{tc} has an inhibitory effect on $sDA_{300,50\%}$ of the terrace classrooms facing each orientation, and the effects on the east-facing and north-facing classrooms are more obvious. In addition, when the classrooms' geometry is the same, the south-facing classrooms have the highest daylight sufficiency, followed by west-facing classrooms, and the east- and north-facing classrooms are relatively low. For $UDI_{100-2000}$, the geometry parameters that significantly impact classrooms facing different orientations vary greatly. H_w , H_{tc} , WWR, and WFR showed significant negative and positive correlations with $UDI_{100-2000}$ in south-facing and north-facing classrooms, respectively.
2. For east- and north-facing terrace classrooms, enlarging W_{tc} and H_{tc} can effectively improve the daylighting performance, so it can be set to the maximum. In addition, when W_{tc} and H_{tc} are greater than 22 m and 3.4 m, respectively, and D_{tc} is less than 14 m, the sufficiency of the ambient daylight available is preferred ($sDA_{300,50\%} \geq 0.75$). For south-facing terrace classrooms, W_{tc} can be maximized to enhance the overall natural lighting. When H_{tc} is greater than 3.1 m, the daylight sufficiency increases with the increase in H_{tc} , but the cumulative time of available illuminance for natural lighting decreases. In addition, when W_{tc} and H_{tc} are greater than 17 m and 3.1 m, respectively, and D_{tc} is less than 15 m, daylight sufficiency is preferred. For west-facing terrace classrooms, W_{tc} can be maximized. In addition, when W_{tc} and H_{tc} are greater than 19 m and 3.4 m, respectively, and D_{tc} is less than 14 m, daylight sufficiency is preferred. Therefore, when designing the interior space geometry of the terrace classroom, attention should be focused upon grasping the appropriate size relationship between D_{tc} , W_{tc} , and H_{tc} in different orientations.
3. The addition of H_w helps improve daylight sufficiency in the terrace classrooms facing each orientation. When the H_w of south- and west-facing classrooms is greater than or equal to 2 m and the H_w of east- and north-facing classrooms is greater than or equal to 2.4 m, daylight sufficiency is preferred. In addition, for north-facing classrooms, adding H_w can increase the cumulative time of the available illuminance for natural lighting, so H_w can be maximized to enhance the overall daylighting performance. For south-facing classrooms, when H_w is greater than 1.8 m, $UDI_{100-2000}$ decreases with the increase in H_w , which is not conducive to the improvement of the overall daylighting performance. Compared with H_w , W_w introduces fewer effects on daylighting quality in terrace classrooms. When the east-facing and north-facing classrooms' W_w is greater than or equal to 4.1 m and the west-facing W_w is greater than or equal to 1.7 m, the sufficiency of the available ambient daylight is preferred. For south-facing and west-facing terrace classrooms, appropriately increasing W_{wbw} is conducive to improving the cumulative time of the available illuminance for natural lighting, and it is best when W_{wbw} is 0.9 m. There is a significant positive correlation between H_{ws} and $UDI_{100-2000}$ in east-, west-, and north-facing terrace classrooms. For east- and west-facing classrooms, H_{ws} should be larger than the indoor desktop height.

With the increase in WWR and WFR, the $sDA_{300,50\%}$ of the terrace classrooms facing each orientation always reflected an upward trend, and south-facing and north-facing terrace classrooms' $UDI_{100-2000}$ reflected a trend that first increased and then decreased. To improve the overall daylighting performance, the WWR and WFR of the south-facing classroom should be 0.3–0.5 and 0.11–0.14, respectively, and the WWR and WFR of the north-facing classroom should be 0.6–0.7 and 0.14–0.20, respectively.

4. Taking the interior space and window geometry parameters of the terrace classrooms as the independent variables, the prediction models of the $sDA_{300,50\%}$ and $UDI_{100-2000}$ of the terrace classrooms facing each orientation were constructed, and the model's fit was high and had significant statistical significance. The prediction model can provide an accurate quantitative evaluation of the daylighting performance of the terrace classrooms of universities in severe cold regions.

Author Contributions: Z.L. and Y.J. contributed to the article equally and should be regarded as co-first authors. Z.L. conceived the paper and designed the numerical study; Y.J., Y.F. and H.Z. performed the numerical simulation; Y.J., Y.F., H.Z., C.Z. and X.C. analyzed the data and created the figures.; Y.J., Y.F. and H.Z. drafted the paper; Z.L. revised the paper. All authors have read and agreed to the published version of the manuscript.

Funding: This work was financially supported by the National Training Program of Innovation and Entrepreneurship for Undergraduates (Grant Number: 220244), the Fundamental Research Program of the Education Department of Liaoning Province (Grant Number: LJKQZ2021006), the Liaoning Social Science Planning Fund Project (Grant Number: L22CGL012), the Fundamental Research Funds for the Central Universities (Grant Number: N2111001), and the National Training Program of Innovation and Entrepreneurship for Undergraduates (Grant Number: 230244).

Data Availability Statement: The data presented in this study are available on request from the authors.

Conflicts of Interest: The authors declare no conflict of interest.

References

1. Haddad, S.; Synnefa, A.; Marcos, M.Á.P.; Paolini, R.; Delrue, S.; Prasad, D.; Santamouris, M. On the potential of demand-controlled ventilation system to enhance indoor air quality and thermal condition in Australian school classrooms. *Energy Build.* **2021**, *238*, 110838. [\[CrossRef\]](#)
2. Heschong, L.; Manglani, P.; Wright, R.; Peet, R.; Howlett, O. Windows and Classrooms: Student Performance and the Indoor Environment. In Proceedings of the ACEEE Summer Study, Pacific Grove, CA, USA, 22–27 August 2004.
3. Roche, L.; Dewey, E.; Littlefair, P. Occupant reactions to daylight in offices. *Light. Res. Technol.* **2000**, *32*, 119–126. [\[CrossRef\]](#)
4. Galasiu, A.D.; Veitch, J.A. Occupant preferences and satisfaction with the luminous environment and control systems in daylight offices: A literature review. *Energy Build.* **2006**, *38*, 728–742. [\[CrossRef\]](#)
5. Cheung, H.; Chung, T. A study on subjective preference to daylight residential indoor environment using conjoint analysis. *Build. Environ.* **2008**, *43*, 2101–2111. [\[CrossRef\]](#)
6. Lim, Y.-W.; Kandar, M.Z.; Ahmad, M.H.; Ossen, D.R.; Abdullah, A.M. Building façade design for daylighting quality in typical government office building. *Build. Environ.* **2012**, *57*, 194–204. [\[CrossRef\]](#)
7. Ghisi, E.; Tinker, J.A. An Ideal Window Area concept for energy efficient integration of daylight and artificial light in buildings. *Build. Environ.* **2005**, *40*, 51–61. [\[CrossRef\]](#)
8. Susorova, I.; Tabibzadeh, M.; Rahman, A.; Clack, H.L.; Elnimeiri, M. The effect of geometry factors on fenestration energy performance and energy savings in office buildings. *Energy Build.* **2013**, *57*, 6–13. [\[CrossRef\]](#)
9. ALee, J.W.; Jung, H.J.; Park, J.Y.; Lee, J.B.; Yoon, Y. Optimization of building window system in Asian regions by analyzing solar heat gain and daylighting elements. *Renew. Energy* **2013**, *50*, 522–531.
10. Omar, O.; Garcia-Fernández, B.; Fernández-Balbuena, A.; Vázquez-Moliní, D. Optimization of daylight utilization in energy saving application on the library in faculty of architecture, design and built environment, Beirut Arab University. *Alex. Eng. J.* **2018**, *57*, 3921–3930. [\[CrossRef\]](#)
11. Fan, Z.; Liu, M.; Tang, S. A multi-objective optimization design method for gymnasium facade shading ratio integrating energy load and daylight comfort. *Build. Environ.* **2022**, *207*, 108527. [\[CrossRef\]](#)
12. Huang, X.; Wei, S.; Zhu, S. Study on Daylighting Optimization in the Exhibition Halls of Museums for Chinese Calligraphy and Painting Works. *Energies* **2020**, *13*, 240. [\[CrossRef\]](#)

13. Li, D.H.W.; Lo, S.M.; Lam, J.C.; Yuen, R.K.K. Daylighting Performance in Residential Buildings. *Arch. Sci. Rev.* **1999**, *42*, 213–219. [[CrossRef](#)]
14. Sun, C.Y.Y.; Han, Y.S. Parametric Daylight Performance Simulation Research of Mezzanine Space in Office Buildings in Severe Cold Regions. *J. Hum. Settl. West China* **2021**, *36*, 24–30.
15. Krüger, E.L.; Fonseca, S.D. Evaluating daylighting potential and energy efficiency in a classroom building. *J. Renew. Sustain. Energy* **2011**, *3*, 063112. [[CrossRef](#)]
16. Al-Dossary, A.M.; Kim, D.D. A Study of Design Variables in Daylight and Energy Performance in Residential Buildings under Hot Climates. *Energies* **2020**, *13*, 5836. [[CrossRef](#)]
17. Dabe, T.J.; Adane, V.S. The impact of building profiles on the performance of daylight and indoor temperatures in low-rise residential building for the hot and dry climatic zones. *Build. Environ.* **2018**, *140*, 173–183. [[CrossRef](#)]
18. Acosta, I.; Campano, M.; Molina, J.F. Window design in architecture: Analysis of energy savings for lighting and visual comfort in residential spaces. *Appl. Energy* **2016**, *168*, 493–506. [[CrossRef](#)]
19. Michael, A.; Heracleous, C. Assessment of natural lighting performance and visual comfort of educational architecture in Southern Europe: The case of typical educational school premises in Cyprus. *Energy Build.* **2017**, *140*, 443–457. [[CrossRef](#)]
20. Junaibi, A.A.A.; Zaabi, E.J.A.; Nassif, R.; Mushtaha, E. Daylighting in Educational Buildings: Its Effects on Students and How to Maximize Its Performance in the Architectural Engineering Department of the University of Sharjah. In Proceedings of the 3rd International Sustainable Buildings Symposium (ISBS 2017), Dubai, United Arab Emirates, 15–17 March 2017.
21. Peters, T.; D’Penna, K. Biophilic Design for Restorative University Learning Environments: A Critical Review of Literature and Design Recommendations. *Sustainability* **2020**, *12*, 7064. [[CrossRef](#)]
22. Ashrafian, T.; Moazzen, N. The impact of glazing ratio and window configuration on occupants’ comfort and energy demand: The case study of a school building in Eskisehir, Turkey. *Sustain. Cities Soc.* **2019**, *47*, 101483. [[CrossRef](#)]
23. Goia, F.; Haase, M.; Perino, M. Optimizing the configuration of a facade module for office buildings by means of integrated thermal and lighting simulations in a total energy perspective. *Appl. Energy* **2013**, *108*, 515–527. [[CrossRef](#)]
24. Wong, N.H.; Istiadji, A.D. Effect of external shading devices on daylighting penetration in residential buildings. *Light. Res. Technol.* **2004**, *36*, 317–333. [[CrossRef](#)]
25. Pellegrino, A.; Cammarano, S.; Savio, V. Daylighting for Green Schools: A Resource for Indoor Quality and Energy Efficiency in Educational Environments. *Energy Procedia* **2015**, *78*, 3162–3167. [[CrossRef](#)]
26. de Rubeis, T.; Nardi, I.; Muttillio, M.; Ranieri, S.; Ambrosini, D. Room and window geometry influence for daylight harvesting maximization—Effects on energy savings in an academic classroom. *Energy Proc.* **2018**, *148*, 1090–1097. [[CrossRef](#)]
27. Mangkuto, R.A.; Rohmah, M.; Asri, A.D. Design optimisation for window size, orientation, and wall reflectance with regard to various daylight metrics and lighting energy demand: A case study of buildings in the tropics. *Appl. Energy* **2016**, *164*, 211–219. [[CrossRef](#)]
28. Galal, K.S. The impact of classroom orientation on daylight and heat-gain performance in the Lebanese Coastal zone. *Alex. Eng. J.* **2019**, *58*, 827–839. [[CrossRef](#)]
29. Lakhdari, K.; Sriti, L.; Painter, B. Parametric optimization of daylight, thermal and energy performance of middle school classrooms, case of hot and dry regions. *Build. Environ.* **2021**, *204*, 108173. [[CrossRef](#)]
30. Ekasiwi, S.N.N.; Antaryama, I.G.N.; Krisdianto, J.; Ulum, M.S. Correlation of classroom typologies to lighting energy performance of academic building in warm-humid climate (case study: ITS Campus Sukolilo Surabaya). *IOP Conf. Series Earth Environ. Sci.* **2018**, *126*, 012049. [[CrossRef](#)]
31. Freewan, A.A.; Al Dalala, J.A. Assessment of daylight performance of Advanced Daylighting Strategies in Large University Classrooms; Case Study Classrooms at JUST. *Alex. Eng. J.* **2020**, *59*, 791–802. [[CrossRef](#)]
32. Milone, D.; Pitruzzella, S.; Franzitta, V.; Viola, A.; Trapanese, M. Energy savings through integration of the illuminance natural and artificial, using a system of automatic dimming: Case study. In Proceedings of the 2nd International Conference on Advanced Materials Design and Mechanics (ICAMDMD 2013), Kuala Lumpur, Malaysia, 17–18 May 2013; p. 253.
33. Davidsson, H.; Perers, B.; Karlsson, B. Performance of a multifunctional PV/T hybrid solar window. *Sol. Energy* **2010**, *84*, 365–372. [[CrossRef](#)]
34. GB50033-2013; Standard for Daylighting Design of Buildings. China Architecture & Building Press: Beijing, China, 2013. (In Chinese)
35. Weather China. Available online: <http://www.weather.com.cn/forecast/history.shtml?areaid=101070101&month=11> (accessed on 25 November 2022).
36. Mohsenin, M.; Hu, J. Assessing daylight performance in atrium buildings by using Climate Based Daylight Modeling. *Sol. Energy* **2015**, *119*, 553–560. [[CrossRef](#)]
37. ElBatan, R.M.; Ismaeel, W.S. Applying a parametric design approach for optimizing daylighting and visual comfort in office buildings. *Ain Shams Eng. J.* **2021**, *12*, 3275–3284. [[CrossRef](#)]
38. IES LM-83-12; Approved Method: IES Spatial Daylight Autonomy (SDA) and Annual Sunlight Exposure (ASE). Illuminating Engineering Society (IES): New York, NY, USA, 2012.
39. Wang, M. *Research on Top Daylighting Design of Classrooms in Primary and Secondary Schools in Guangdong Based on Visual Health*; South China University of Technology: Guangzhou, China, 2018. (In Chinese)

40. Nabil, A.; Mardaljevic, J. Useful daylight illuminances: A replacement for daylight factors. *Energy Build.* **2006**, *38*, 905–913. [[CrossRef](#)]
41. Rastegari, M.; Pournaseri, S.; Sanaieian, H. Daylight optimization through architectural aspects in an office building atrium in Tehran. *J. Build. Eng.* **2021**, *33*, 101718. [[CrossRef](#)]
42. Xue, Y.; Liu, W. A Study on Parametric Design Method for Optimization of Daylight in Commercial Building's Atrium in Cold Regions. *Sustainability* **2022**, *14*, 7667. [[CrossRef](#)]
43. Kharvari, F. An empirical validation of daylighting tools: Assessing radiance parameters and simulation settings in Ladybug and Honeybee against field measurements. *Sol. Energy* **2020**, *207*, 1021–1036. [[CrossRef](#)]
44. Ma, Q.S.; Fukuda, H. Parametric office building for daylight and energy analysis in the early design stages. In Proceedings of the Conference on Urban Planning and Architectural Design for Sustainable Development (UPADSD), Lecce, Italy, 14–16 October 2015; pp. 818–828.
45. Energyplus, Weather Data. Available online: <https://energyplus.net/weather> (accessed on 17 December 2022).
46. *Architectural Design Data Set*; China Architecture & Building Press: Beijing, China, 2019.
47. *GB 50099-2011*; Code for Design of School. China Architecture & Building Press: Beijing, China, 2011. (In Chinese)
48. Xu, Z.; Wang, T.; Li, C.; Bao, L.; Ma, Q.; Miao, Y. Brief Introduction to the Orthogonal Test Design. *J. Libr. Inf. Sci.* **2002**, *12*, 148–150. (In Chinese)
49. *GB 50352-2019*; Uniform Standard for Design of Civil Buildings. China Architecture & Building Press: Beijing, China, 2019. (In Chinese)
50. Liu, R.; Zhang, Y.; Wen, C.; Tang, J. Study on the design and analysis methods of orthogonal experiment. *Exp. Technol. Manag.* **2010**, *27*, 52–59. (In Chinese) [[CrossRef](#)]
51. *GB/T 5699-2017*; Method of Daylighting Measurements. Standardization Administration: Beijing, China, 2017. (In Chinese)
52. Leng, H.; Chen, X.; Ma, Y.; Wong, N.H.; Ming, T. Urban morphology and building heating energy consumption: Evidence from Harbin, a severe cold region city. *Energy Build.* **2020**, *224*, 110143. [[CrossRef](#)]
53. Nault, E.; Moonen, P.; Rey, E.; Andersen, M. Predictive models for assessing the passive solar and daylight potential of neighborhood designs: A comparative proof-of-concept study. *Build. Environ.* **2017**, *116*, 11–16. [[CrossRef](#)]
54. Voll, H.; Seinre, E. A method of optimizing fenestration design for daylighting to reduce heating and cooling loads in offices. *J. Civ. Eng. Manag.* **2014**, *20*, 714–723. [[CrossRef](#)]
55. Allam, A.S.; Bassioni, H.A.; Kamel, W.; Ayoub, M. Estimating the standardized regression coefficients of design variables in daylighting and energy performance of buildings in the face of multicollinearity. *Sol. Energy* **2020**, *211*, 1184–1193. [[CrossRef](#)]
56. Deng, X.; Wang, M.; Fan, Z.; Liu, J. Dynamic daylight performance oriented design optimizations for contemporary reading room represented deep open-plan spaces. *J. Build. Eng.* **2022**, *62*, 105145. [[CrossRef](#)]
57. Rupp, R.F.; Ghisi, E. Assessing window area and potential for electricity savings by using daylighting and hybrid ventilation in office buildings in southern Brazil. *Simulation* **2017**, *93*, 935–949. [[CrossRef](#)]
58. Zheng, C. *Study on Parametric Design of Natural Lighting Performance of University Building in Hubei Province*; Yangtze University: Jingzhou, China, 2021. [[CrossRef](#)]
59. Zhang, Q. *Research on Daylighting Design of Teaching Buildings in Hanzhong Area*; Xi'an University of Architecture and Technology: Xi'an, China, 2021. [[CrossRef](#)]
60. Fela, R.F.; Utami, S.S.; Mangkuto, R.A.; Suroso, D.J. The Effects of Orientation, Window Size, and Lighting Control to Climate-Based Daylight Performance and Lighting Energy Demand on Buildings in Tropical Area. In Proceedings of the International Building Performance Simulation Association International Conference and Exhibition, Rome, Italy, 2–4 September 2019. [[CrossRef](#)]

Disclaimer/Publisher's Note: The statements, opinions and data contained in all publications are solely those of the individual author(s) and contributor(s) and not of MDPI and/or the editor(s). MDPI and/or the editor(s) disclaim responsibility for any injury to people or property resulting from any ideas, methods, instructions or products referred to in the content.